

Signaling between periglomerular cells reveals a bimodal role for GABA in modulating glomerular microcircuitry in the olfactory bulb

Pirooz Victor Parsa^{a,b}, Rinaldo David D'Souza^{a,b,1}, and Sukumar Vijayaraghavan^{a,b,2}

^aDepartment of Physiology and Biophysics, University of Colorado School of Medicine, Aurora, CO 80045 and ^bNeuroscience Program, University of Colorado School of Medicine, Aurora, CO 80045

Edited by Charles F. Stevens, The Salk Institute for Biological Studies, La Jolla, CA, and approved June 23, 2015 (received for review December 22, 2014)

In the mouse olfactory bulb glomerulus, the GABAergic periglomerular (PG) cells provide a major inhibitory drive within the microcircuit. Here we examine GABAergic synapses between these interneurons. At these synapses, GABA is depolarizing and exerts a bimodal control on excitability. In quiescent cells, activation of GABA_A receptors can induce the cells to fire, thereby providing a means for amplification of GABA release in the glomerular microcircuit via GABA-induced GABA release. In contrast, GABA is inhibitory in neurons that are induced to fire tonically. PG-PG interactions are modulated by nicotinic acetylcholine receptors (nAChRs), and our data suggest that changes in intracellular calcium concentrations triggered by nAChR activation can be amplified by GABA release. Our results suggest that bidirectional control of inhibition in PG neurons can allow for modulatory inputs, like the cholinergic inputs from the basal forebrain, to determine threshold set points for filtering out weak olfactory inputs in the glomerular layer of the olfactory bulb via the activation of nAChRs.

nicotinic | excitatory GABA | interneurons | cholinergic | normalization

The balance of excitation and inhibition is critical for the normal functioning of brain networks. Timed inhibition of principal neurons modulates circuit output and contributes to network synchrony and oscillation. GABAergic interneurons play a key role in regulating these network properties (1, 2). Recent findings (e.g., ref. 3), however, have compelled us to move away from a simple view of transmission in the brain, in which glutamate and GABA represent the major excitatory and inhibitory transmitter systems, to a more nuanced interpretation of their roles.

GABAergic neurotransmission has both inhibitory and excitatory effects in the CNS. Whereas the inhibitory actions of GABA on principal neurons in different brain regions have been examined extensively, studies of excitatory GABA have focused mostly on the developmental aspects of neuronal growth and synapse formation (4, 5). Recent evidence suggests that GABA can be excitatory in mature neurons as well (with the term “mature” here referring to neurons that are integral parts of established brain networks) (3, 6).

Dynamic GABAergic signaling between inhibitory interneurons is less well understood. The common assumption is that GABAergic signaling between these interneurons would lead to disinhibition of principal neurons in a circuit. Excitatory GABA signaling between these interneurons, on the other hand, could serve as a means for amplification of principal cell inhibition. A combination of the two could effectively buffer interneuron firing rates and possibly normalize circuit output in a given area (7).

The modularity in brain circuits allows for application of principles gleaned from the study of one defined circuit to other circuits as well. In the olfactory bulb (OB) glomerulus, the GABAergic periglomerular (PG) cells provide a large fraction of the inhibitory drive for information transfer between the olfactory nerve (ON) and mitral cells (MCs), the principal neurons. In this system, the existence of PG-PG synapses has been demonstrated (8), and GABA has been suggested to be depolarizing, yet inhibitory, on these neurons (9). Whether these synapses participate in glomerular

signaling either during odor input or during neuromodulation of glomerular output is not yet known.

In this paper, we report that GABAergic connections between PG cells have a bimodal effect on excitation depending on the previous activity state of the neurons. Excitation of PG cells by GABA can lead to amplification of glomerular inhibition via GABA-induced GABA release (GIGR). GABA release from PG cells modulates glomerular output on the activation of nicotinic acetylcholine receptors (nAChRs), wherein weak signals from the ON are filtered out while stronger ones are transmitted (10). Our results suggest that bimodal signaling by GABA could be important in determining set points for inhibition thresholds in the glomerular microcircuit.

Results

GABA Type A Receptor Activation Raises Intracellular Free Calcium Levels. We first tested whether GABA was depolarizing in a population of juxtglomerular (JG) neurons. Slices were loaded with fura-2AM. To isolate GABAergic signals, loaded slices were incubated with glutamate receptor (GluR) blockers [10 μ M 6,7-dinitroquinoxaline-2,3-dione (DNQX), 50 μ M (2*R*)-amino-5-phosphonopentanoate (APV), and 500 μ M (*S*)- α -methyl-4-carboxyphenylglycine (MCPG), to block AMPA and NMDA receptors and metabolic GluRs, respectively] and TTx. GABA (100 μ M–1 mM) was applied locally via a puffer pipette. Calcium signals were monitored from JG neurons.

Brief (1–5 s) application of GABA to OB glomeruli from 12- to 18-d-old mice resulted in rapid calcium transients (Fig. 1*A, i*).

Significance

Excitation-driven inhibition is one mechanism for manipulating gain control in brain microcircuits. Here we show that interactions between GABAergic interneurons in the glomerulus in the olfactory bulb can, in a dynamic fashion, regulate inhibition of circuit output. GABA is depolarizing on these interneurons; however, depending on the activity state of these neurons, it can be excitatory or inhibitory, thereby providing a bimodal regulation of inhibition. In the olfactory bulb, activation of nicotinic acetylcholine receptors can drive glutamate-dependent GABAergic mechanisms that allow for timed filtering of incoming inputs. These mechanisms can serve to normalize inhibition across the glomerular layer by cholinergic activation, taking into account both behavioral states and the activity history of individual glomeruli.

Author contributions: P.V.P., R.D.D., and S.V. designed research; P.V.P. and R.D.D. performed research; P.V.P., R.D.D., and S.V. analyzed data; and P.V.P., R.D.D., and S.V. wrote the paper.

The authors declare no conflict of interest.

This article is a PNAS Direct Submission.

¹Present address: Department of Anatomy and Neurobiology, Washington University School of Medicine, St. Louis, MO 63110.

²To whom correspondence should be addressed. Email: sukumar.v@ucdenver.edu.

This article contains supporting information online at www.pnas.org/lookup/suppl/doi:10.1073/pnas.1424406112/-DCSupplemental.

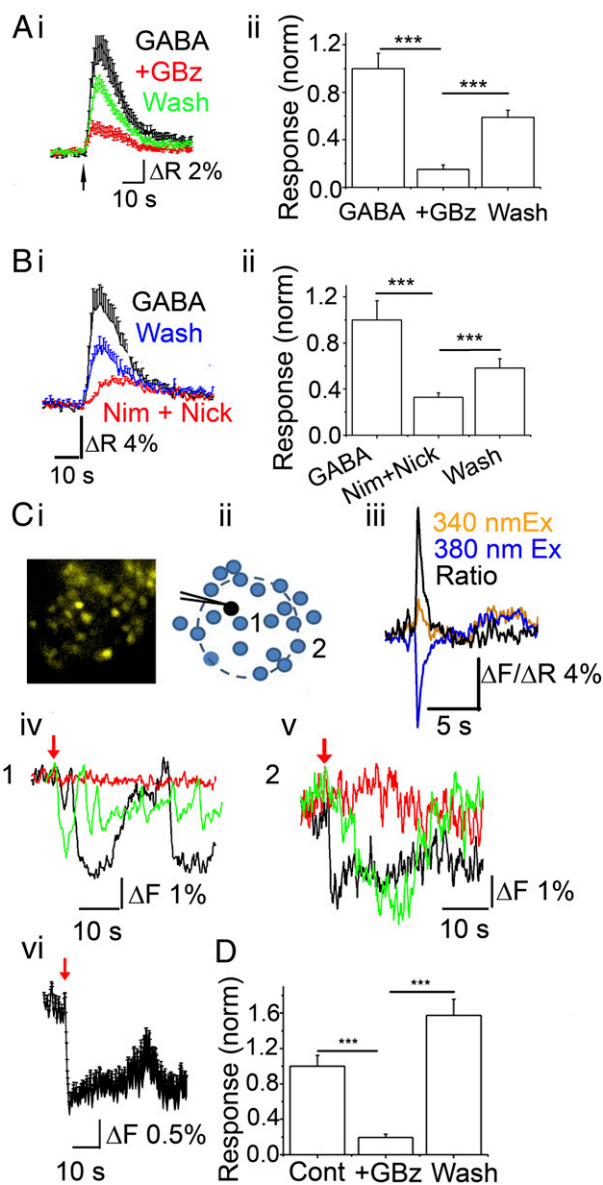


Fig. 1. Both exogenous and endogenous GABA induce GABA_A receptor-mediated calcium transients in a population of JG neurons. (A) (i) Averaged trace (\pm SEM) of calcium transients from JG neurons in response to a 5-s application of 1 mM GABA in the presence of 1 μ M TTX, 50 μ M DNQX, and 100 μ M APV. Black, GABA; red, in the presence of 20 μ M GBz (+GBz); green, wash. (ii) Data quantification from *i* ($n = 63$ cells from four experiments). GBz potently inhibited GABA-induced calcium transients ($P < 10^{-8}$ compared with GABA alone, paired *t* test), which was reversed on washout of the antagonist ($P < 10^{-7}$ compared with +GBz). (B) (i) A 5-s application of 1 mM GABA triggers VGCC-dependent calcium transients in a population of JG neurons. Average trace (\pm SEM) from control (GABA; black), in the presence of 20 μ M nimodipine and 500 μ M nickel (Nim + Nick; red), and wash (blue). (ii) Quantification of data ($n = 51$ cells, three experiments; $P < 0.001$ for GABA and wash compared with Nim + Nick). *** $P < 0.0005$, paired *t* test. (C and D) Calcium transients in response to depolarization of a single PG cell. (C) Fura-2AM-loaded cells were imaged before and after delivery of a single 100-ms voltage step to a PG neuron in the presence of 10 μ M DNQX and 50 μ M APV. (i) Image of a fura-2AM-loaded glomerulus. (ii) Cartoon depicting the recorded PG cell (black) and surrounding JG cells that respond with calcium transients to the depolarizing step (blue). (iii) Calcium transient from the patched PG cell (loaded with 200 μ M bis-fura-2 hexapotassium salt) on a 100-ms voltage step. The orange trace represents changes from the 340-nm excitation; blue trace, changes from the 380-nm excitation; black trace, changes in the 340 nm/380 nm ratio. (iv) Changes in fluorescence from 380-nm excitation from a single cell (cell labeled 1 in D) eliciting an oscillatory calcium transient on PG cell depolarization alone (black), in the presence of 20 μ M GBz (red), and wash (green). (v) Fluorescence from 380-nm excitation changes from another cell (cell labeled 2 in D) eliciting a calcium transient on PG cell depolarization (black), in the presence of 20 μ M GBz (red), and wash (green). (vi) Average response (\pm SEM) from all responding cells ($n = 21$) in the glomerulus. (D) Data from four independent experiments. Cells surrounding the patched PG neuron show calcium transients that are blocked by 20 μ M GBz (+GBz; $P < 0.0001$). On washout, the response recovered ($P < 0.0001$, compared with +GBz).

Incubating the slices with 20 μ M gabazine (GBz) reduced the fluorescence (integrated over the response) to $15 \pm 3.7\%$ of the control responses ($n = 63$ cells from three experiments; $P < 10^{-8}$, paired *t* test) which was partially reversed (to $55 \pm 6\%$ of the control response) after a 10-min washout ($n = 63$; $P < 10^{-7}$, paired *t* test compared with GBz) (Fig. 1A, ii). We then confirmed that GABA-mediated calcium transients were not unique to young mice. From five experiments, JG cells from 75- to 90-d-old mouse OBs also responded to GABA with an increase in $[Ca]_i$ (Fig. S1), indicating that age is not a determining factor.

We then confirmed that the calcium signals obtained from GABA type A receptor (GABA_AR) activation resulted from depolarization of the cells by testing the contribution of voltage-gated calcium channels (VGCCs). Incubating the slices with 50 μ M nimodipine and 500 μ M nickel reduced the calcium response to $33 \pm 3\%$ of control ($n = 51$ cells from three experiments; $P < 0.0005$; paired *t* test), which was partly reversed upon washout (Fig. 1B, i and ii). To confirm VGCC blockade, we measured the effects of the blockers on calcium responses to 70 mM KCl on the same cells. The VGCC antagonists reduced the response to a 1-s application of 70 mM KCl to $45 \pm 3\%$ of control ($P < 0.0005$).

Based on these results, we asked whether endogenously released GABA from PG cells could result in calcium changes in surrounding neurons, potentially via PG-PG interactions. We loaded slices with fura-2AM (Fig. 1C, i). We held PG neurons under a whole-cell voltage clamp using CsCl-based internal solutions containing 10 mM GABA, 200 μ M bis-fura-2 hexapotassium salt, and 200 μ M Alexa Fluor 594 hydrazide (to confirm the identity of the recorded PG cell). GluR currents were blocked using 10 μ M DNQX and 50 μ M AP-5. A 100-ms voltage step was applied from -70 mV to 0 mV. Images were acquired at 2–7 Hz. GBz-sensitive, slow “self-inhibitory” currents were observed following the voltage step (119 ± 42 pA; $n = 4$ cells out of 7).

We measured calcium changes from all JG neurons within a glomerulus before and for 45 s after the voltage step. Results are shown in Fig. 1C. Following the voltage step, surrounding JG neurons showed calcium transients. Surprisingly, responses were not confined to neurons in the vicinity of the voltage-clamped neurons, but were widespread across the glomerulus (Fig. 1C, i–vi). On average, $60 \pm 14\%$ of all JG neurons that were loaded with fura-2AM responded with calcium transients ($n = 4$ experiments). We did not investigate the possible spread of the signal across glomeruli in this study. The onset of the calcium response in all responding neurons occurred with a ≤ 1 -s delay in the voltage step, suggesting fast propagation of the signal. Incubating cells with 10 μ M GBz reduced the response by $87 \pm 2.4\%$ (data from four experiments; $P < 0.0001$, paired *t* test), which was reversed after 15 min of washing (Fig. 1D). The recovered response was $52 \pm 10\%$ larger on average than the first response ($P < 0.05$, paired *t* test). Whether this increase indicates some tonic regulation of basal calcium levels by ambient GABA remains to be investigated.

The foregoing results are consistent with the idea that GABA is depolarizing in PG cells. The surprising finding that depolarizing a single PG neuron can raise calcium levels in most JG neurons raises the possibility that GABA is excitatory and can propagate signals across PG cells.

GABA Is Excitatory on PG Cells. Smith and Jahr (9) suggested that depolarization by GABA nevertheless blocks firing in PG neurons

(green). (v) Fluorescence from 380-nm excitation changes from another cell (cell labeled 2 in D) eliciting a calcium transient on PG cell depolarization (black), in the presence of 20 μ M GBz (red), and wash (green). (vi) Average response (\pm SEM) from all responding cells ($n = 21$) in the glomerulus. (D) Data from four independent experiments. Cells surrounding the patched PG neuron show calcium transients that are blocked by 20 μ M GBz (+GBz; $P < 0.0001$). On washout, the response recovered ($P < 0.0001$, compared with +GBz).

via shunt inhibition. To determine whether PG neurons can fire on activation of GABA receptors, we performed cell-attached recordings from PG cells using recording pipettes containing 200 μM Alexa Fluor 594 hydrazide. These cells were initially identified by their size and the fact that none of them showed spontaneous bursts of action potentials (APs), a characteristic of the glutamatergic external tufted (ET) cells. The idea that PG cells exhibit very little to no spontaneous firing is consistent with recent studies demonstrating the same *in vivo* (11, 12). All experiments were done in the presence of the aforementioned GluR blockers. In six out of six cells, where we successfully broke through into a whole-cell configuration, their identity was further confirmed morphologically (small size, short dendritic arbors; Fig. 2A). Brief applications of 25–50 μM GABA resulted in firing of PG cells (Fig. 2A). GABA-mediated changes in PG cell firing were completely blocked by incubating the slice in 20 μM GBz ($n = 4$). Transient GABA-induced firing in these neurons lasted an average of 3.2 ± 0.85 s, with an average frequency of 6.3 ± 2 Hz ($n = 9$ cells). An additional four cells fired one or two APs on GABA application.

Our results suggest that GABA is excitatory on these neurons; however, it is possible that GABA is inhibitory in PG cells but the cells themselves are under a tonic inhibition from other GABA-sensitive neurons. Thus, application of GABA would result in disinhibition of PG cells by removal of this tonic inhibition. Such a scenario implies that under current-clamp conditions, application of GABA should result in depolarization even under conditions in which GABA is hyperpolarizing in the recorded neuron. We performed whole-cell current-clamp recordings from PG cells, using intracellular solutions (K-gluconate based; $E_{\text{Cl}} = -108$ mV) that would make GABA hyperpolarized in the recorded cell (Fig. 2B). The resting membrane potential (RMP), determined immediately after going whole cell, averaged -55 ± 3 mV ($n = 7$ cells). Brief applications of 100 μM GABA resulted in no membrane depolarizations, as would be predicted if the excitatory actions of GABA arose from disinhibition of a tonically inhibited cell ($n = 5$).

We examined whether activation of the hyperpolarization activated current (I_h), known to be present in MCs (13) and a subset of PG cells (14), contributes to PG cell firing. Cell-attached recordings were carried out on PG cells in the presence and absence of 30 μM ZD 7288, an I_h blocker (15, 16). In the presence of the inhibitor, application of 25 μM GABA still elicited firing (mean firing frequency, 1.35 ± 0.37 Hz in controls vs. 2.28 ± 0.73 Hz after a 15-min treatment with ZD 7288; $n = 5$ cells; $P = 0.3$) (Fig. S2 A and B). Consistent with our current-clamp experiments (Fig. 2B), these results suggest that I_h activation does not drive the cells above their firing threshold. The lack of depolarization in the current-clamp recordings also makes it unlikely that other forms of rebound depolarization contribute to the excitatory effects of GABA.

Having ruled out disinhibition or rebound depolarization, we conducted measurements of the reversal potential for GABA-evoked currents (E_{GABA}) in PG cells. Perforated patch recordings were carried out using K-gluconate-based solutions containing gramicidin D (Methods). GABA currents were measured at various holding potentials (Fig. 2C). From a total of six cells, the mean E_{GABA} was calculated to be -49 ± 2 mV. RMPs were obtained from seven cells. Of these, six cells had a mean RMP of -60 ± 2 mV, and one cell had an RMP of -45 mV. This finding suggests that most PG cells rest approximately 10 mV negative to E_{GABA} , thereby making GABA depolarizing on these neurons. The observed E_{GABA} would result from an intracellular chloride concentration of approximately 19 mM, assuming that bicarbonate does not significantly affect the GABA reversal potential. This compares with intracellular chloride concentrations of 15 mM observed in cerebellar interneurons where GABA is depolarizing (7) and 25 mM in newborn hippocampal neurons (17).

In 10 cells, either with the first GABA application or after repeated application of the agonist, the originally silent neuron went into a persistent firing mode firing at an average frequency of

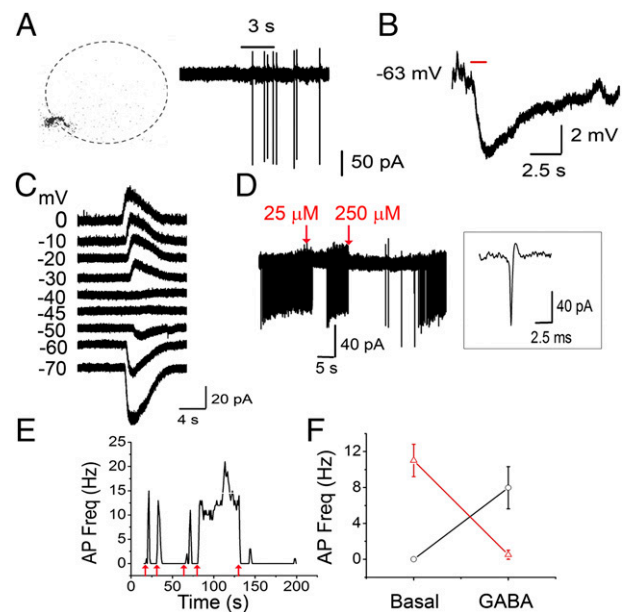


Fig. 2. Bimodal actions of excitatory GABA. (A) (Left) PG cell filled with Alexa Fluor 594 hydrazide after cell-attached recording. (Right) Cell-attached recording from the same cell. The cell was held at 0 holding current. A 3-s (black bar) 25 μM GABA application (in the presence of 10 μM DNQX and 50 μM APV) triggers a transient burst of APs. (B) A PG cell under whole-cell current-clamp ($I = 0$). A 1-s application of 100 μM GABA results in hyperpolarization of the membrane potential, arguing against disinhibition. No rebound depolarization was observed. The RMP was -63 mV. (C) Responses to a 3-s application of 50 μM GABA were recorded at various holding potentials (from -70 mV to 0 mV) using gramicidin D perforated patch recordings. E_{GABA} in this cell was at approximately -45 mV. (D) Long-lasting bursts of APs were triggered by application of 25 μM GABA. Firing was inhibited in response to application of both 25 μM and 250 μM GABA (red arrows) for 3 s. (Inset) Expanded trace showing a single event. (E) Frequency plot of a PG cell responding to 25 μM GABA (red arrows) either with a small burst of APs or a long burst of APs that was shunted (at the fourth arrow). Same cell as in D. (F) Average response plot of all cells representing bimodality of GABA responses. PG neurons that were silent were excited (black; $n = 6$). Neurons that were induced to fire continuously after GABA application were inhibited (red; $n = 7$).

8.9 ± 2 Hz ($n = 7$; Fig. 2D–F) after the agonist was removed. When GABA was applied to a tonically firing PG cell, its effect was to silence the neuron for a brief period ($n = 6$; Fig. 2F). A 1-s application of 25–50 μM GABA transiently silenced the neuron (Fig. 2D), which recovered after washout of the agonist.

A parsimonious interpretation of our results (Figs. 1 and 2) is that activation of GABA_ARs results in depolarization-driven calcium flux via the opening of VGCCs and drives the cell above its firing threshold. Given that it is possible to evoke both transient and continuous firing in the same PG cell, this is less likely to reflect different subpopulations of these neurons rather than differences in active conductances, including those activated by calcium entry. Whether PG cell firing, induced by previous activation of GABA_ARs, provides the necessary total conductance for effective shunt inhibition or whether there are rapid changes in intracellular chloride concentrations remains to be determined. The bidirectional effect of GABA also will prevent a potential positive feedback loop that might lead to runaway excitation of the PG cell population.

GABAergic Signaling Among PG Cells via GIGR. To further demonstrate that GABA released from a PG neuron can result in amplified GABA release within the glomerular network via PG–PG interactions (i.e., GIGR), we asked whether exogenous GABA, applied at a distance, can give rise to spontaneous GABAergic postsynaptic currents (sGSPCs). A PG neuron was held under

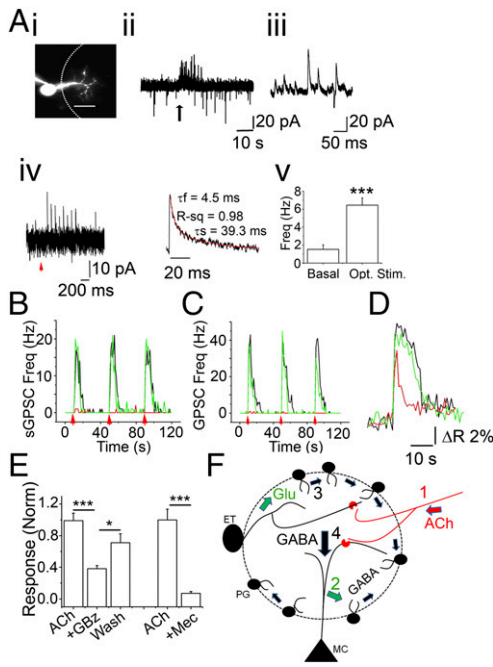


Fig. 4. nAChR activation results in glutamate-dependent increase in the frequency of sGPSC on PG cells. (A) (i) A PG cell loaded with Alexa Fluor 488 dextran to identify its dendritic arborization within a glomerulus. (Scale bar: 10 μ m.) (ii) A 5-s application of 1 mM ACh/At at the arrow results in a barrage of sGPSCs recorded at -30 mV. (iii) Expanded trace showing individual sGPSCs from the barrage in ii. (iv) Recordings of a PG neuron from a ChAT-ChR2 mouse. (Left) Optical stimulation (473 nm) of cholinergic fibers for 10 ms at 10 Hz results in a barrage of sGPSCs in the recorded PG cell. (Right) Expanded example of an averaged sGPSC from iv. (v) Averaged sGPSC frequencies under basal (basal) and stimulated (opt. stim.) conditions ($n = 9$; $P < 0.005$, paired t test). (B) Frequency plot representing sGPSC frequency change owing to ACh/At applications (red arrows) control (black), 5 μ M Mec (red), and wash (green). ACh/At-mediated increase in sGPSC frequencies arises from activation of heteromeric nAChRs. Mec abolishes nAChR-mediated increases in sGPSC frequencies. (C) Frequency plot representing sGPSC frequency change owing to ACh/At applications (red arrows) in control (black), GluR blockers (red), and wash (green). GluR blockers (20 μ M DNQX + 100 μ M D-APV + 1 mM MCPG) reversibly abolish ACh/At-induced barrage of sGPSCs at -30 mV. (D) Calcium transient from a JG neuron in response to 1 mM ACh/At. The agonist elicits a large calcium transient (black trace) that is significantly attenuated after application of 20 μ M GBz (red trace) in a reversible manner (wash; green trace), consistent with the idea that nAChR-dependent GABA release contributes to PG cell calcium signals. (E) Compiled data from 24 cells from three experiments showing response to nAChR activation (ACh), block by 20 μ M GBz (GBz), and washout (wash). *** $P < 10^{-8}$, ACh vs. +GBz; * $P < 0.05$, +GBz vs. wash. Similarly the nAChR-mediated calcium transients were blocked by 5 μ M Mec (+Mec). *** $P < 10^{-5}$. Significance was calculated using the paired t test. (F) A model for GIGR. Functional nAChRs (red crescents) are expressed on MC primary dendrites and on ET cells (10, 19). Release of ACh from basal forebrain cholinergic neurons (red; 1) activates the nAChRs, resulting in glutamate release onto a population of PG cells (green; 2). Excitation of PG cells in turn releases GABA on to adjacent PG cells, resulting in propagation of this excitation via GIGR (black, small arrows; 3). This results in amplified GABA release and inhibition of all MCs in the microcircuit (black, large arrow; 4), filtering weak inputs from the ON. Runaway excitation of PG cells is prevented by GABA_AR-mediated inhibition of PG cell firing, thereby establishing a finite set point for glomerular inhibition.

ON stimulation, when the cell was held at 0 mV (Fig. S34, i). The mean delay to the first sGPSC was 15 ± 2.6 ms ($n = 6$). Increases in sGPSC frequencies were observed both in cells that showed discernible EPSCs on ON stimulation and those that did not (Fig. S34, i and B). The average sGPSC frequency on stimulation (measured from onset to a 90% decay in binned frequency distribution; Fig. S34, iii) was 2.7 ± 0.5 Hz ($n = 16$). The average peak frequency was 7.2 ± 1.2 Hz, and the average duration of the sGPSC burst was 4.76 ± 0.5 s ($n = 6$ cells). The mean frequency

increase was lower when the ON was stimulated with low frequencies (two pulses at 2 Hz; 0.9 ± 0.3 Hz; $n = 13$; $P < 0.01$) (Fig. S3D).

As expected, the increase in sGPSCs on PG cells after ON stimulation was excitation-driven, presumably via glutamate release onto PG cells from the ON, ET cells, or MCs. Incubating the slices with 10 μ M DNQX and 50 μ M APV abolished the OMPChR2-driven increase in sGPSC in a reversible manner (89.4% block; $n = 4$; $P < 0.05$) (Fig. S3A, iii and C).

Based on the GluR-dependence of the GPSC increase in PG cells during both nAChR modulation and ON stimulation, we predicted that activation of nAChRs should increase glutamate release onto PG cells as well. We measured changes in the frequencies of glutamatergic synchronous EPSCs (sEPSCs) on nAChR activation in PG neurons. Surprisingly, only a fraction of PG cells ($\sim 35\%$; 16 out of 46 cells) that we recorded from exhibited a significant increase in the frequency of sEPSCs on focal application of 1 mM ACh/At (Fig. S4; significance for increases in individual cells established by the Kolmogorov–Smirnov test for interevent intervals between sGPSCs). Whether this reflects the reported heterogeneity in glutamatergic inputs onto the PG cells (20, 21) remains to be determined. For cells exhibiting a significant increase in sEPSCs, the mean sEPSC frequency increased from 1.52 ± 0.46 Hz to 11.05 ± 2.25 Hz ($n = 16$; $P < 0.001$, paired t test). This ACh-mediated increase in sEPSC frequencies in PG cells was also abolished by 5 μ M Mec (92.6% blockade for sEPSCs; $n = 5$; $P < 0.05$, paired t test). Cells that showed sEPSC frequency increases also showed robust bursts of sGPSCs (included in the aforementioned analyses of the sGPSC effects).

The involvement of PG–PG signaling in nAChR modulation implies that GIGR could serve as a means of amplifying glomerular inhibition in response to receptor activation (Fig. 4F). If this is the case, then a simple prediction, based on our data obtained thus far, would be that GABA_ARs contribute to nAChR-mediated calcium transients in JG neurons. Calcium transients in response to 1 mM ACh/At were recorded from JG neurons from slices loaded with fura-2AM. Consistent with the data presented above and previous laboratory work (10, 19), activation of nAChRs produced robust calcium transients that were blocked on incubation with 5 μ M Mec ($86 \pm 5.6\%$ block; $n = 35$ cells; $P < 10^{-5}$, paired t test) (Fig. 4E). Importantly, 20 μ M GBz significantly blocked nAChR-mediated increases in $[Ca]_i$ (Fig. 4D). From a total of 38 cells from three experiments, loaded with fura-2AM, 24 cells showed a decrease in 100 μ M ACh/At-mediated ΔR in the presence of GBz (mean inhibition, $61\% \pm 3.8\%$; $P < 10^{-8}$, paired t test) (Fig. 4E). A small fraction of the JG neurons showed an increase in response to the GABA_AR block (response in the presence of the blocker, $190\% \pm 50\%$ of ACh/At alone; $n = 5$, $P < 0.05$) (Fig. 4E). Whether these results indicate tonic inhibition by GABA of ET cells and other non-PG cells in the glomerulus or is a consequence of the bimodality of GABAergic effects on PG cells remains to be determined. Our findings suggest that GABA release from JG neurons contributes to nAChR-mediated calcium transients, consistent with the idea that GIGR can serve to amplify glomerular inhibition in response to circuit excitation.

Discussion

This study makes two important observations. The first of these is that PG–PG interactions are prevalent in the glomerular microcircuitry. Models of OB function need to incorporate these synapses and their unique ability to dynamically regulate glomerular inhibition. The combination of excitatory GABA and GIGR provides a previously unidentified mechanism for the regulation of the transfer function across the glomerulus. The second observation is that these interactions participate in modulation by cholinergic centrifugal inputs.

Connections between GABAergic interneurons are thought to play a role in shaping spatial and temporal features of circuit

